Control of Carbene Reactivity by Crystals. A Highly Selective 1,2-H Shift in the Solid-to-Solid Reaction of 1-(4′-Biphenylyl)-2-phenyldiazopropane to (*Z*)-1-(4′-Biphenylyl)-2-phenylpropene

Steve H. Shin, Deniz Cizmeciyan, Amy E. Keating, Saeed I. Khan, and Miguel A. Garcia-Garibay*

Contribution from the Department of Chemistry and Biochemistry, University of California, Los Angeles, California 90095

Received September 23, 1996[⊗]

Abstract: Ruby red polycrystalline samples of 1-(4′-biphenylyl)-2-phenyldiazopropane (**1a**) efficiently transform into colorless (*Z*)-1-(4′-biphenylyl)-2-phenylpropene [(*Z*)-**3a**] in up to 96% yield in a highly selective photochemical solid-to-solid reaction. The solid state reaction was shown to proceed via a carbene intermediate, and it was formulated as a 1,2-H shift with unprecedented stereoselectivity. It was shown that irradiation of **1a** in inert solvents gives products via 1,2-H shifts [(*Z*)-**3a** and (*E*)-**3a**] and 1,2-Ph migrations [(*Z*)-**4a** and (*E*)-**4a**] in yields that vary strongly with the polarity of solvent. Irradiation of **1a** in ethanol gave similar products along with ethers **5a** from insertion of the carbene into the EtO−H bond.

I. Introduction

In their pioneering work, Doetschman and Hutchison showed that the crystalline solid state may exert a very high degree of control over the chemical fate of diphenylcarbene.[1] Using crystalline 1,1-diphenylethylene as a host and a combination of X-ray crystallographic analysis and EPR and ENDOR spectroscopies, they were able to describe two competing bimolecular reactions with a high degree of structural and kinetic accuracy. Given the potential demonstrated by their early work, it is surprising that no other reports have followed in what seems to be an area of great potential for organic chemistry. A possible deterrent for such studies comes from the uncertainty of an *a priori* knowledge of suitable packing arrangements required for bimolecular, carbene−carbene, carbene−olefin, or carbene−precursor reactions that may or may not give rise to alkenes, cyclopropanes and azines.[2] Thus, in order to carry out a systematic study of carbene reactivity in the crystalline solid state with no need for specific packing arrangements, we have begun an investigation of unimolecular carbene reactions. On the basis of expectations of crystallinity, structural variability, and experimental convenience, we chose as a starting point a reaction model involving the intermediacy of 1,2-diarylalkylidenes (**2**). As other arylalkylcarbenes, these highly reactive intermediates are capable of undergoing 1,2-H and 1,2-alkyl shifts as well as 1,2-Ph migrations (Scheme 1). We envisioned the formation of carbenes **2** in crystals of their readily available 1,2-diaryldiazoalkane precursors **1**. With several examples, we have found that the solid-state reactivity of 1,2-diaryldiazoalkanes is quite general. However, it is the purpose of this paper to present a very detailed analysis of the solid-state reactivity of 1-(4′-biphenylyl)-2-phenyl-diazopropane, **1a** (Ar = 4′-biphenylyl, R = Me, and Ar′ = Ph), which represents in many ways an ideal model system. Compound **1a** gives high-melting crystals with excellent diffraction properties, and a detailed comparison of results obtained in solution and in the solid state demonstrates an unprecedented degree of control by the crystalline medium.[6] We have found that the reaction may proceed at ambient temperatures entirely in the solid phase with a very high selectivity and up to 95% conversion.

Scheme 1

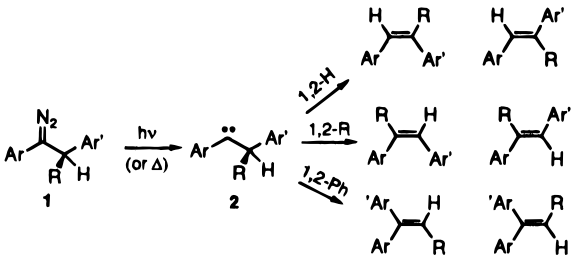

II. Results and Discussion

The photochemistry of 1,2-diaryldiazoalkanes has been studied in detail in fluid solutions, frozen solvents, and amorphous glassy matrices by the groups of Pomerantz and Whitherup[3] and Platz and Tomioka[4] and by ourselves.[5] We will describe here the first detailed analysis carried out in the crystalline solid state.[6] It has been shown that 1,2-diaryldiaz-

[⊗] Abstract published in *Advance ACS Abstracts,* February 1, 1997.

(1) Doetschman, D. C.; Hutchison, C. A. *J. Chem. Phys.* **1972**, *56*, 3964−3982.

(2) For some leading reviews on carbene chemistry see: (a) Brinker, U. H. *Advances in Carbene Chemistry*; JAI Press, Inc.: New York, 1994. (b) Nickon, A. *Acc. Chem. Res.* **1993**, *26*, 84−89. (c) Platz, M. S. In *Kinetics and Spectroscopy of Carbenes and Biradicals*; Platz, M. S., Ed.; Plenum Press: New York, 1990; pp 143−212. (d) Schuster, G. B. *Adv. Phys. Org. Chem.* **1986**, *22*, 311−362.

(3) Pomerantz, M.; Witherup, T. H. *J. Am. Chem. Soc.* **1973**, *95*, 5977−5988.

(4) (a) Platz, M. S. In *Kinetics and Spectroscopy of Carbenes and Biradicals*; Platz, M. S., Ed.; Plenum Press: New York, 1990; pp 143−212. (b) Tomioka, H.; Hayashi, N.; Sugiura, T.; Izawa, Y. *J. Chem. Soc., Chem. Commun.* **1986**, 1364−1366. (c) Tomioka, H.; Hayashi, N.; Izawa, Y.; Senthilnathan, V. P.; Platz, M. S. *J. Am. Chem. Soc.* **1983**, *105*, 5053−5057. (d) Tomioka, H.; Ueda, H.; Kondo, S.; Izawa, Y. *J. Am. Chem. Soc.* **1980**, *102*, 7817−7818.

(5) (a) Garcia-Garibay, M. A. *J. Am. Chem. Soc.* **1993**, *115*, 7011−7012. (b) Garcia-Garibay, M. A.; Theroff, C.; Shin, S. H.; Jernelius, J. *Tetrahedron Lett.* **1993**, *52*, 8415−8418.

(6) For a communication of this work see: Shin, H. S.; Keating, A. E.; Garcia-Garibay, M. A. *J. Am. Chem. Soc.* **1996**, *118*, 7626−7627.

S0002-7863(96)03322-7 CCC: $14.00

Scheme 2

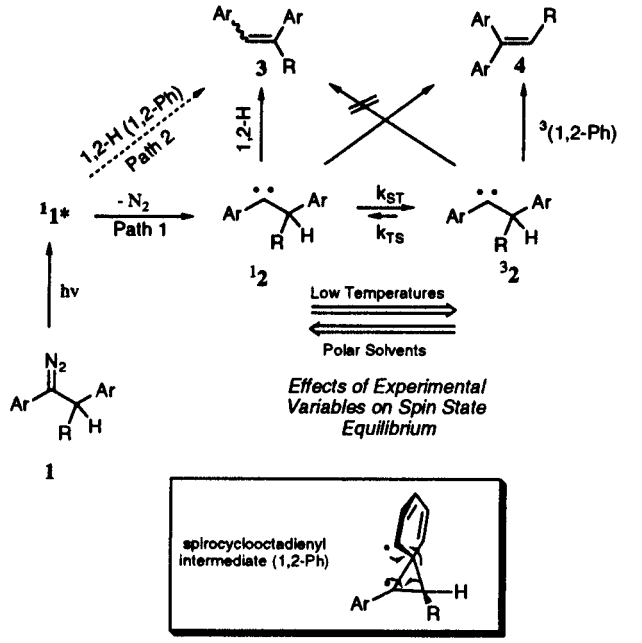

oalkanes display a very rich solution photochemistry where product ratios depend strongly on temperature, solvent polarity, and physical state. Most experimental observations reported in the literature regarding the chemistry of 1,2-diaryldiazoalkanes can be explained in terms of a reaction scheme originally proposed by Tomioka (Scheme 2). The proposed mechanism assumes quantitative denitrogenation of ^{1}**1*** (Scheme 2, path 1) to produce a 1,2-diphenylalkylidene **2**.[4] Recent reports with other arylalkyldiazoalkanes and diazirines suggest that formation of products may also occur from the excited state of the nitrogenated compound (path 2).[7] Work in progress in our group with similar compounds suggests that path 2 in 1,2-diarylalkylidenes contributes with values that range between 0 and 30%.[8]

In analogy with several thoroughly studied diarylcarbenes (e.g., diphenylcarbene),[9,10] it has been proposed that the singlet excited state of **1** forms the singlet carbene ^{1}**2**, which can rapidly equilibrate with the lower energy triplet ^{3}**2** (Scheme 2). The main products in inert solvents include stilbenes **3** and 1,1-diarylethenes **4**, the formation of which can be formulated in terms of well-known carbenic 1,2-H shifts[2b,10] and 1,2-Ph migrations, respectively.[11] Changes in the relative yields of **3** and **4** as a function of temperature and solvent polarity can be consistently explained in terms of environmental perturbation of a sensitive spin-state equilibrium.[5] This model makes the reasonable assumption that 1,2-diphenylalkylidenes have properties similar to those of well-known diaryl carbenes.[9] Reactions are assumed to occur from a spin state pre-equilibrated carbene that displays spin-state specific reactivity as suggested by the Skell−Woodworth[12] rules and the Bethell[13] mechanism. It has been proposed that ^{1}**2** can undergo fast 1,2-H shifts (and slower 1,2-Ph migrations), while ^{3}**2** can only undergo 1,2-Ph migrations by way of a bridged spirocyclooctadienyl biradical (Scheme 2).[4a,b] Pronounced changes in the **3**:**4** ratio as a function of temperature have been interpreted in terms of changes in the equilibrium populations of the two spin states.[4c] Similarly, changes in the **3**:**4** ratio as a function of solvent polarity have been interpreted in terms of a solvent-induced stabilization of the polar singlet carbene that affects the singlet−triplet energy gap, ΔG_{ST}, as well as the spin-state equilibrium constant.[5]

This mechanistic interpretation requires that temperature and solvent effects on the intrinsic reaction rates $k_{1,2-H}$ and $k_{1,2-Ph}$ are smaller than on the equilibrium dynamics of the spin states of the carbene, k_{ST} and k_{TS}. While limited experimental information suggests that these conditions may be possible, the mechanism in Scheme 2 is only tentative and alternative interpretations of experimental effects cannot be ruled out. This brief analysis stresses the complexity of a system where at least three precursors (^{1}**1***, **2S**, and **2T**), two of which may equilibrate (**2S** and **2T**), may be involved in the formation of each of the observed products.

Table 1. Literature Data for Some 1,2-Diaryldiazoalkanes and 1,2-Diarylalkylidenes

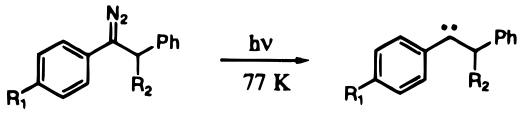

compd	R_1	R_2	mp (°C)	D^a (h/c)	E^a (h/c)	ref
1a	Ph	Me	93	0.470	0.029	this work
1b	H	H	oil	0.497	0.029	17
1c	H	Me	oil[b]	0.498	0.027	4c
1d	H	Et	oil	na	na	5

[a] Zero field splitting parameters for the corresponding carbene. [b] We could obtain poor quality crystals that melt at 19 °C.

Scheme 3

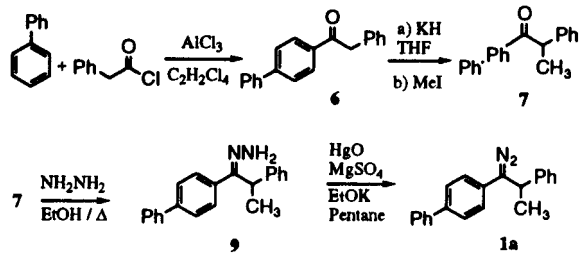

(1) Synthesis and Characterization of 1-(4′-Biphenylyl)-2-phenyldiazopropane, 1a. While studies of several 1,2-diaryldiazoalkanes (e.g., **1b**−**1d**) have been reported in the literature (Table 1), these compounds have been described as thermally unstable viscous oils.[4a,c] We found that a 4-phenyl substituent on the 1,2-diaryldiazopropane chromophore results in a high-melting and highly crystalline solid that can be stored indefinitely in the dark at −20 °C without traces of chemical decomposition.

The diazo compound **1a** [1-(4′-biphenylyl)-2-phenyldiazopropane] was prepared from biphenyl and phenylacetyl chloride by the sequence of reactions shown in Scheme 3. Compounds **6** and **7** were isolated in 71% and 93% yield, respectively, after purification by column chromatography. The hydrazone **8** was obtained in 67% yield by crystallization from ethanol, and

(7) (a) Platz, M. S.; White, W. R.; Modarelli, D. A.; Celebi, S. *Res. Chem. Intermed.* **1994**, *20*, 175−193. (b) Celebi, S.; Leyva, S.; Modarelli, D. A.; Platz, M. S. *J. Am. Chem. Soc.* **1993**, *115*, 8613−8620. (c) Modarelli, D. A.; Morgan, S.; Platz, M. S. *J. Am. Chem. Soc.* **1992**, *114*, 7034−7041. (d) White, W. R., III; Platz, M. S. *J. Org. Chem.* **1992**, *57*, 2841−2846.

(8) Motschiedler, K. R.: Toscano, J. P.; Garcia-Garibay, M. A. *Tetrahedron Lett.*, in press.

(9) (a) Closs, G. L.; Rabinow, B. E. *J. Am. Chem. Soc.* **1976**, *98*, 8190−8198. (b) Eisenthal, K. B.; Turro, N. J.; Sitzmann, E. V.; Gould, I. R.; Hefferon, G.; J., L.; Cha, Y. *Tetrahedron* **1985**, *41*, 1543−1554. (c) Griller, D.; Nazran, A. S.; Scaiano, J. C. *Tetrahedron* **1985**, *41*, 1525−1530. (d) Schuster, G. B. *Adv. Phys. Org. Chem.* **1986**, *22*, 311−362.

(10) (a) Schaefer, H. F., III. *Acc. Chem. Res.* **1979**, *12*, 288−296. (b) Liu, M. T. H. *Acc. Chem. Res.* **1994**, *27*, 287−294.

(11) (a) Liu, M. T. H. *J. Phys. Org. Chem.* **1993**, *6*, 696−698. (b) Nickon, A.; Bronfenbrenner, J. K. *J. Am. Chem. Soc.* **1982**, *104*, 2022−2023.

(12) Woodworth, R. C.; Skell, P. S. *J. Am. Chem. Soc.* **1959**, *81*, 3383−3386.

(13) (a) Bethell, D.; Hayes, J.; Newall, A. R. *J. Chem. Soc., Perkin Trans. 2* **1974**, 1307−1312. (b) Bethell, D.; Stevens, G.; Tickle, P. *J. Chem. Soc., Chem. Commun.* **1970**, 792−794.

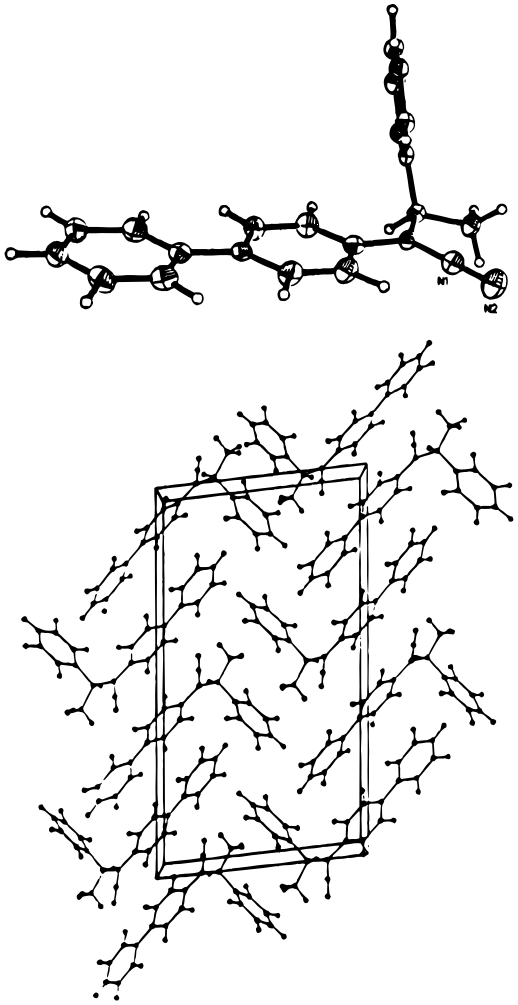

Figure 1. X-ray structure and packing diagram of compound **1a**.

oxidation of **8** with HgO in pentane as a solvent in the presence of $MgSO_4$ and EtOK yielded pure diazo **1a** in 81% yield. Ruby red crystals of **1a** were obtained by slow evaporation of pentane at −20 °C as long needles. While differential scanning calorimetry (DSC) traces with slow heating rates showed slow thermal decomposition (*vide infra*), a sharp melting point of 93−94 °C was obtained on a hot stage apparatus when melting was accomplished with rapid heating rates. Compound **1a** was fully characterized by spectroscopic methods both in solution and in the solid state. The spectroscopic signatures of the diazo group[14] were observed in its characteristic red color with a λ_{max} at 515 nm (Figure 3), a sharp stretching band at 2033 cm^{-1} in the IR spectrum, and a very shielded signal at 79.4 ppm in the ^{13}C NMR.

Single-crystal X-ray diffraction revealed the space group $P2_1/c$ with one molecule per asymmetric unit. The details of data collection and refinement are included in the Supporting Information. The molecular structure of **1a** is characterized by having the 4′-biphenyl, diazo, and methyl substituents in a nearly coplanar arrangement, while the α-hydrogen and phenyl groups are located above and below this plane with torsion angles N_2=C−C−H and N_2=C−C−Ph of 127° and −115.5°, respectively (Figure 1). The planarity between diazo and the biphenylyl system probably comes from maximized conjugation between the two π-systems while the coplanarity of methyl and diazo groups may be understood in terms of dipole-induced dipole interactions such as those proposed to account for the

(14) Patai, S. *The Chemistry of the Diazonium and Diazo Groups*; John Wiley & Sons: New York, 1978.

Scheme 4

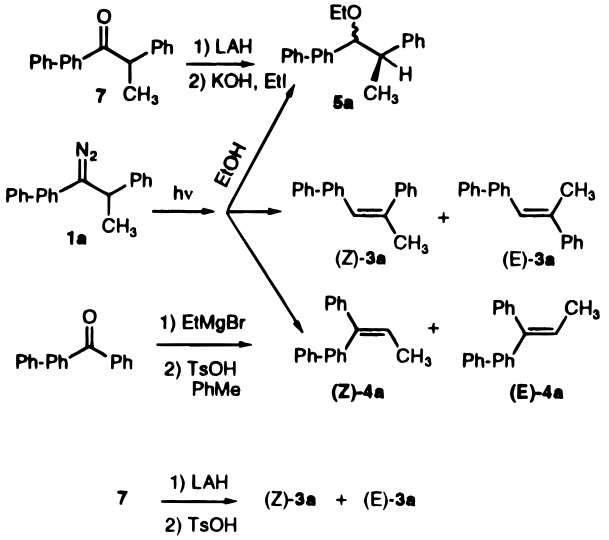

Table 2. Product Distribution from Photolysis of **1a** in Several Solvents[a]

solvent	(*Z*)-**3a**	(*E*)-**3a**	**4a** (*Z*+*E*)	**5a**
hexane	16	10	53 + 21	0
acetonitrile	39	18	32 + 11	0
ethanol	22	10	4 + 1	64

[a] Irradiation at 0 °C with λ > 380 nm.

conformational preferences of π-systems with α-alkyl groups (ketones, alkenes, arenes).[15]

The packing diagram of **1a** viewed along the short *b* axis (Figure 1) depicts columns of molecules running along the crystallographic *c* axis (vertical axis) with pairwise centrosymmetric interactions that position the diazo group of one molecule directly above the biphenylyl group of another. Face to face interactions between phenyl groups of neighboring columns and edge-to-face interactions between biphenylyl and phenyl substituents may also be discerned in the packing structure.

(2) Solution Photolysis and Product Characterization. Photochemical irradiation of diazo **1a** in deoxygenated hexanes and acetonitrile led to formation of both *E* and *Z* isomers of 1-(4′-biphenylyl)-2-phenylpropene (**3a**) and 1-(4′-biphenylyl)-1-phenylpropene (**4a**) (Scheme 4). No products from the much slower 1,2-Me shift reaction or intramolecular C−H insertion were observed. The relative product yields established by GC analysis were highly solvent dependent (Table 2). It was also shown in a different experiment that irradiation of **1a** in pure ethanol leads to compounds **3a** and **4a** along with 64% yield of ethers **5a**. The identification of olefins **3a** and **4a** and ethers **5a** was carried out by coinjection of authentic samples independently synthesized from 4-phenylbenzophenone and from 1-(4′-biphenylyl)-2-phenylpropanone (**7**) using conventional functional group transformations as indicated in Scheme 4.

Compounds (*E*)-**3a** and (*Z*)-**3a** were separated by fractional recrystallization, but numerous attempts to separate (*E*)-**4a** and (*Z*)-**4a** by fractional crystallization and by preparative TLC and HPLC on various solid supports were unsuccessful. The stereochemical identity of (*E*)-**3a** and (*Z*)-**3a** was suggested by ^1H NMR NOE measurements, and it was unambiguously established by X-ray diffraction analysis of the (*Z*)-isomer, which was also the predominant photoproduct in the solid state. The X-ray structure of (*Z*)-**3a** was solved in the space group $P2_1/c$ with two independent molecules per asymmetric unit

(15) (a) Wiberg, K., B. *J. Am. Chem. Soc.* **1986**, *108*, 5817−5822. (b) Wiberg, K. B.; Murcko, M. A. *J. Comput. Chem.* **1988**, *9*, 488−494.

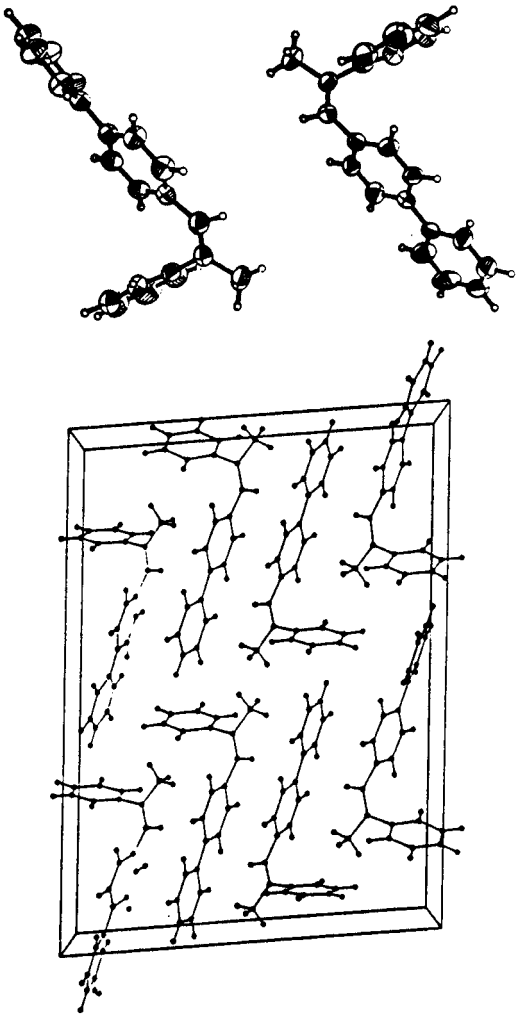

Figure 2. X-ray molecular structures of compound (*Z*)-**3a** showing the two conformers present in the asymmetric unit and the packing diagram along the *b* axis.

(Figure 2). The details of data collection and refinement are included in the Supporting Information.

As observed with other 1,2-diaryldiazoalkanes, product ratios in solution are highly solvent dependent. However, in order to obtain reliable product ratios care must be exercised in the selection of excitation wavelengths. In order to prevent cis−trans isomerization[16] by secondary photochemical reactions of the stilbene (**3**) and diarylethene chromophores (**4**), all irradiations were carried out with $\lambda > 380$ nm. It can be seen in the UV spectrum in Figure 3 that irradiation through a 380 nm cutoff filter results in exclusively excitation of the weak ($\epsilon_{max} = 57$ L M^{-1} cm^{-1}) and long-wavelength n,π^* absorption ($\lambda_{max} = 515$ nm) of the diazo chromophore. It was shown that product ratios under these conditions are constant as a function of irradiation time and reaction progress. It was also shown that stereochemically pure (or enriched) samples of these compounds remained photostable upon irradiation with $\lambda > 380$ nm.

(3) Measurements in Low-Temperature Glasses. Product selectivity in solution is rather low, and variations in product yields in Table 2 are complex. In order to explain these observations, the identity of the precursor(s) of the observed products was investigated. Evidence in support of pathway 1 was obtained by irradiation of **1a** in rigid glasses at 77 K in the cavity of the ESR spectrometer. We observed a triplet signal with zero-field splitting parameters ($D = 0.470$ and $E = 0.029$ cm^{-1}) and kinetic behavior nearly identical to those reported by Trozzolo for 1,2-diphenylethylidene (**1b**)[17] and by Platz and Tomioka for 1,2-diphenylpropylidene[4c] (**1c**, Table 1). The lifetime of this triplet in MCH glasses was relatively short (few seconds), and its detection required continuous illumination at 77 K. This signal has been assigned to carbene ^{3}**2a**, which we suggest is the ground state of **2a**.

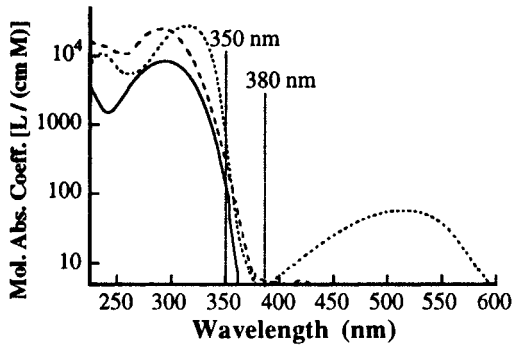

Figure 3. UV−vis spectra of compounds **1a** (dotted line), (*Z*)-**3a** (dashed line), and (*E*)-**3a** (full line). The cutoff wavelengths of glass filters used in various experiments are indicated by vertical lines.

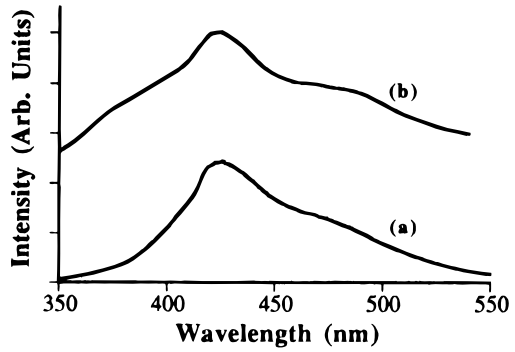

Figure 4. Fluorescence spectra in methylcyclohexane at 77 K of (a) purified (*Z*)-**3a** and (b) samples of **1a** irradiated at 77 K to give primarily (*Z*)-**3a** (not corrected for detector response).

Following the detection of carbene **2a** by EPR, we attempted the detection of its T−T fluorescence at 77 K. While the T−T fluorescence of numerous diarylcarbenes and naphthylcarbenes has been observed over the last 30 years,[18] the emission of arylalkylcarbenes remains to be documented.[19] While we could not observe a transient signal that we could assign to carbene **2a**, we noticed the growth of a strong emission signal at $\lambda =$ 440 nm. We found that the spectrum obtained by irradiation of diazo **1a** at 77 K was nearly identical to that obtained from purified samples of stilbene (*Z*)-**3a** (Figure 4).

It was shown that irradiation of **1a** at 77 K in methylcyclohexane gives rise to alkenes (*Z*)-**3a** and (*E*)-**3a** in *ca.* 45 and 15% yields, respectively, along with a mixture of products from reaction with the matrix (*ca.* 40%).[4] In agreement with previous observations by Tomioka *et al.*, no products from the sterically demanding 1,2-Ph migration were observed.[4d] It was also shown that the fluorescence of the product mixture corresponded to that of the *cis*- and *trans*-stilbenes (*Z*)-**3a** and (*E*)-**3a**.

Growth of the fluorescence signal of the photoproducts as a function of time offers an opportunity to analyze the kinetics

(16) Turro, N. J. *Modern Molecular Photochemistry*; Benjamin/Cummings Publishing Co.: Menlo Park, 1978; Chapter 12.

(17) Trozzolo, A. M.; Wasserman, E. In *Structure of Arylcarbenes*; Moss, R. A., Jones, M., Jr., Eds.; John Wiley & Sons: New York, 1975; pp 185−206.

(18) (a) Trozzolo, A. M.; Gibbons, W. A. *J. Am. Chem. Soc.* **1967**, *89*, 239−243. (b) Scaiano, J. C.; Weir, D. *Can. J. Chem.* **1988**, *66*, 491−494. (c) Johnston, L. J.; Scaiano, J. C. *Chem. Phys. Lett.* **1985**, *116*, 109−113.

(19) From several arylalkylcarbenes recently analyzed, we have only been able to assign emission from phenyl-*tert*-butylcarbene: Shin, S. H.; Garcia-Garibay, M. A. Unpublished results.

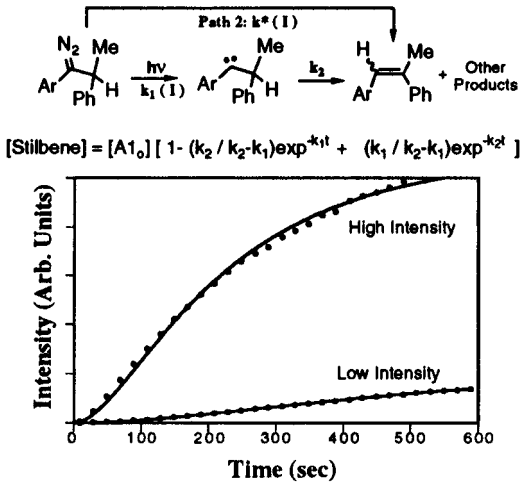

Figure 5. Kinetics of **1a** by fluorescence of the stilbene products as a function of time at two light intensities in ethanol at 77 K (5% of the total data points shown). The line indicates the fit to the kinetic scheme shown on top.

of the reaction (Figure 5). A primary photochemical process is expected to give linear intensity vs. time plots with a reaction velocity proportional to the number of quanta absorbed and to the quantum yield of reaction.[20] In contrast, products from a long-lived intermediate (i.e., several seconds) should be detectable after an induction period, and their formation should continue after illumination is stopped. Thus, the signals of the stilbene products were monitored as a function of time using the spectrofluorimeter to excite both the reactant and the product at $\lambda = 320 \pm 10$ nm. While a strict kinetic analysis was not attempted, signals assigned to the photoproducts (largely stilbene **3a**) grow with the behavior characteristic of a two-step process involving a dark intermediate (Figure 5).[21] The growth of the product fluorescence was fit to the kinetic model shown in Figure 5. The first step [i.e., k_1(I)] represents the generation of the carbene and is light-intensity dependent, while the second step (k_2) represents the overall (thermal) reaction of the carbene. While we assume that the 1,2-H shift occurs from the singlet state, we do not know whether intersystem crossing or reaction from the singlet carbene is rate determining. Variations in light intensity over a factor of 90 accomplished with different slit settings qualitatively reveal the expected dependence of k_1(I). The values of k_2 displayed a smaller intensity dependence, which we postulate may be due to photochemistry of the carbene, as suggested by reports from McMahon and Chapman in their studies of phenylmethylcarbene.[22] The values for k_2 obtained in methylcyclohexane glasses at 77 K in low-intensity experiments are estimated to be *ca*. 0.002−0.005 s^{-1}. These are qualitatively consistent with the EPR measurements where a short carbene lifetime is suggested by the requirement of continuous illumination to maintain an observable spin concentration. To support our assignments, we carried out experiments with deuterated samples of **1a**. Although isotope effects in carbene 1,2-H shift reactions are known to be anomalous,[22,23] we expected that the proposed kinetic scheme would display a primary isotope effect in the second step of the reaction. In fact, a value of $\tau_D/\tau_H = 1.5$ (±0.2) was calculated for the second step when the α-deuterio compound was analyzed. While this value is smaller than expected for a primary isotope effect at this temperature, it is consistent with those reported for other carbene 1,2-H shifts,[22−24] for which there is growing evidence suggesting the involvement of quantum mechanical tunneling.

While the above results provide evidence for product formation via a carbene intermediate in rigid glasses at low temperatures, the involvement of an excited-state reaction of **^{1}1a*** in fluid media at higher temperatures cannot be discounted. Triplet sensitization studies in progress in our group with compounds that bypass **^{1}1a*** suggest that products from the diazo singlet excited state in solution (pathway 2) may have a contribution of *ca*. 30% yield.[8] Nonetheless, with strong evidence for **2a** as an intermediate, the formation of **3a** and **4a** can be formulated in terms of carbenic 1,2-H shifts and 1,2-Ph migrations, respectively, while formation of **5a** (Scheme 4) may be formulated in terms of insertion of **2a** into the polar O−H bond when ethanol is present.[25] If we assume that the excited state of the diazo does not react with the solvent, results in ethanol indicate that at least 64% of the reaction goes through a trappable carbene intermediate.[7] Trends in product yields as a function of solvent polarity are in agreement with the mechanism in Scheme 2.[4,5] We propose that the more polar solvent stabilizes the singlet state and increases its equilibrium population, thus favoring the formation of products **3a** via a singlet 1,2-H shift at the expense of **4a**, which would form primarily via a triplet state 1,2-Ph migration. Polar solvents are also known to stabilize the transition state for 1,2-H reactions,[26] which may also contribute to the changes in product yield observed.

(4) Photolysis in Crystalline Samples of 1a.[27] A large number of solid-state photochemical reports have described studies where the extent of reaction is systematically limited to low conversion values. It is assumed that reactive crystals will degrade at high conversion and the reaction selectivity will be adversely affected. This may be true in many cases. However, studies by Hasegawa *et al.*,[28] Novak *et al.*,[29] and Choi *et al.*[30] have demonstrated that a careful selection of experimental conditions may have important consequences on the progress of the reaction. In particular, excitation at the longest possible wavelengths helps avoid absorption by the photoproduct and ensures the longest possible penetration depth. Photochemical reactions under these conditions probably dissipate less heat, occur in a more homogeneous manner, and have a better opportunity to maintain their crystal control.

(20) Wagner, P. J. In *CRC Handbook of Organic Photochemistry*; Scaiano, J. C., Ed.; CRC Press: Boca Raton, FL, 1989; pp 251−269.

(21) Steinfeld, J. I.; Fransisco, J. S.; Hase, W. L. *Chemical Kinetics and Dynamics*; Prentice Hall: Englewood Cliffs, 1989; Chapter 2.

(22) McMahon, R. J.; Chapman, O. L. *J. Am. Chem. Soc.* **1987**, *109*, 683−692.

(23) (a) Storer, J. W.; Houk, K. N. *J. Am. Chem. Soc.* **1993**, *115*, 10426−10427. (b) Dix, E. J.; Herman, M. S.; Goodman, J. L. *J. Am. Chem. Soc.* **1993**, *115*, 10424−10425.

(24) (a) McMahon, R. J.; Chapman, O. L. *J. Am. Chem. Soc.* **1987**, *109*, 683−692. (b) Moss, R. A.; Ho, G.-J.; Liu, W.; Sierakowski, C. *Tetrahedron Lett.* **1992**, *33*, 4287−4290. (c) Moss, R. A.; Xue, S.; Ma, Y. *Tetrahedron Lett.* **1996**, *30*, 4287−4290. (d) Moss, R. A.; Xue, S.; Ma, Y. *Tetrahedron Lett.* **1996**, *37*, 1929−1932.

(25) (a) Tomioka, H.; Hayashi, N.; Sugiura, T.; Izawa, Y. *J. Chem. Soc., Chem. Commun.* **1986**, 1364−1366. (b) Griller, D.; Liu, M. T. H.; Scaiano, J. C. *J. Am. Chem. Soc.* **1982**, *104*, 5549−5551. (c) Warner, P. M.; Chu, I. S. *J. Am. Chem. Soc.* **1984**, *106*, 5366−5367. (d) Moss, R. A.; Shen, S.; Wlostowski, M. *Tetrahedron Lett.* **1988**, *29*, 6417−6420.

(26) Sugiyama, M. H.; Celebi, S.; Platz, M. S. *J. Am. Chem. Soc.* **1992**, *114*, 966−973.

(27) For some leading reviews in solid-state organic chemistry see: (a) Ramamurthy, V.; Venkatesan, K. *Chem. Rev.* **1987**, *87*, 433−481. (b) Desiraju, G. R. *Organic Solid State Chemistry*; Elsevier: Amsterdam, 1987; p 550. (c) Scheffer, J. R.; Garcia-Garibay, M.; Nalamasu, O. *Org. Photochem.* **1987**, *8*, 249−347. (d) Toda, F. *Acc. Chem. Res.* **1995**, *28*, 480−486. (e) Paul, I. C.; Curtin, D. Y. *Science* **1975**, *187*, 19−26. (f) Schmidt, G. M. J. *Solid State Photochemistry*; Ginsburg, D., Ed.; Verlag Chemie: New York, 1976. (g) Hasegawa, M. *Adv. Phys. Org. Chem.* **1995**, *30*, 117−171.

(28) Chung, C.-M.; Hasegawa, M. *J. Am. Chem. Soc.* **1991**, *113*, 7311−7316.

(29) Enkelmann, V.; Wegner, G.; Novak, K.; Wagener, K. B. *J. Am. Chem. Soc.* **1994**, *115*, 10390−10391.

(30) Choi, T.; Cizmeciyan, D.; Khan, S.; Garcia-Garibay, M. A. *J. Am. Chem. Soc.* **1995**, *118*, 12893−12894.

Scheme 5

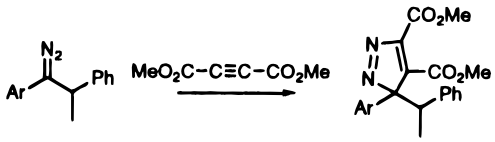

Scheme 6

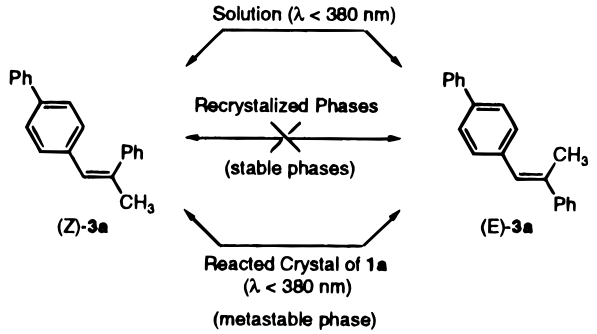

Photolysis of polycrystalline powdered samples and single crystals of **1a** were carried out at 0 °C and at ambient temperatures with a 450 W water-cooled medium-pressure mercury arc Hanovia lamp and with a 1000 W Hg−Xe Oriel lamp. Although consistent results independent of crystal size were obtained at these temperatures, we found that excitation wavelengths have a strong influence on the reaction. Experiments were carried out with cutoff filters with $\lambda > 350$ or $\lambda > 380$ nm to determine the influence of absorption by the product (if any) at the shorter wavelength. Product analyses were carried out by GC as a function of UV exposure. Since the unreacted diazo decomposes thermally in the GC column into the same products obtained by photolysis, all partially reacted samples were treated with excess dimethyl acetylenedicarboxylate (DMAD), which was added to the solution containing the product mixture and the internal standard. It was shown that DMAD removes the diazo compound quantitatively in less than 5 min at ambient temperatures to form (presumably) the corresponding pyrazolines (Scheme 5). Although the latter decompose thermally in the GC column they present no interference because of their different GC retention times.

Results obtained by irradiation at $\lambda > 350$ nm are plotted in Figure 6 (top frame) as reaction progress versus normalized yield, or selectivity, for each of the three products detected [(*Z*)-**3a**, (*E*)-**3a**, and traces of one of the isomers of **4a**]. Irradiation to very low conversion values (ca. 0.5−5%) resulted in the nearly exclusive formation of (*Z*)-**3a** with only traces of (*E*)-**3a** and **4a**. Continued irradiation and product accumulation from *ca*. 5.0% up to 50−60% conversion resulted in decreased reaction selectivity with (*Z*)-**3a** accounting for *ca*. 75−80% of the product mixture. Microscopic analysis of samples as a function of reaction progress showed no liquid phases, although changes in color from red to pink to white were evident as the product accumulated. As shown in the final portion of the graph in Figure 3, a very noticeable change in the selectivity of the reaction occurred between 60 and 100% conversion. Although compound **4a** remained at the trace level, by the time the reaction was nearly complete, compound (*E*)-**3a** had become the major product. Mass balance shows that the rise in the yield of (*E*)-**3a** and the fall in the yield of (*Z*)-**3a** are due to photoisomerization of (*Z*)-**3a**. In fact, this was demonstrated with several control experiments summarized in Scheme 6.

Compound (*Z*)-**3a** was photolyzed in three different media: benzene solution, pure recrystallized samples, and as it is formed in photolyzed crystals of **1a**. In solution, with a Pyrex filter ($\lambda > 290$ nm), the photostationary state is 45% (*Z*)-**3a** and 55% (*E*)-**3a**. With a 350 nm filter, we measured 38% (*Z*)-**3a** and 62% (*E*)-**3a**. With a 380 nm filter we observed no photoisomerization. In recrystallized samples of (*Z*)-**3a** there was no photoisomerization observed with $\lambda > 290$, $\lambda > 350$, or $\lambda > 380$ nm. Finally, a similar set of experiments was carried out with samples of **1a** that had been irradiated with $\lambda > 380$ nm and that contained *ca*. 95% of (*Z*)-**3a** (*vide infra*). In these samples, isomerization was observed when the solid was exposed through cutoff filters that selected for $\lambda > 290$ and $\lambda > 350$ nm, but not when exposed to $\lambda > 380$ nm.

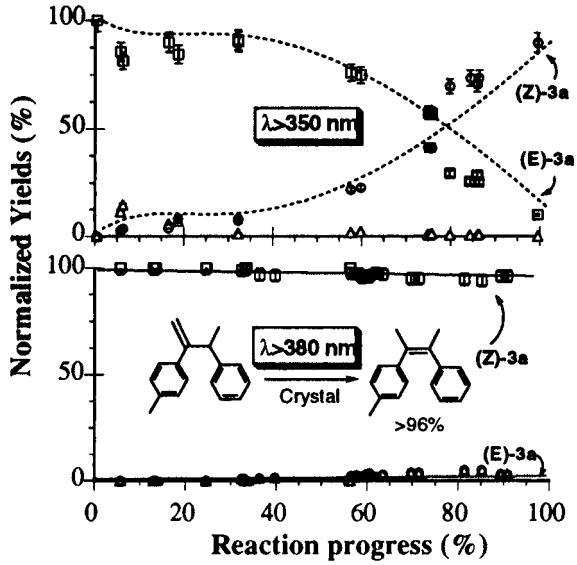

Figure 6. Changes in the normalized yields of (*Z*)-**3a** (squares), (*E*)-**3a** (circles), and **4a** (triangles), as a function of reaction progress upon irradiation of crystalline **1a** at 0 °C with $\lambda > 350$ nm (top frame) and with $\lambda > 380$ nm (bottom frame).

The above results show that the relative yields of compounds (*Z*)-**3a** and (*E*)-**3a** at high conversion reflect their photostationary state in the solid state.[31] The UV absorption spectra of **1a**, (*Z*)-**3a,** and (*E*)-**3a** in the solid parallels their absorption in cyclohexane. Selective excitation of (*Z*)-**3a** occurs with $\lambda > 350$ nm but not with $\lambda > 380$ nm (Figure 3). While cis−trans photoisomerization of alkenes in the solid state is rare, it is not unprecedented.[31] However, differences in reactivity between recrystallized samples of (*Z*)-**3a** and samples obtained by irradiation of crystals of **1a** suggest two entirely different solid phases. As discussed below, samples of "as formed" (*Z*)-**3a** probably exist in a metastable phase that is quite different from the one it crystallizes in under equilibrium conditions.

As expected from the above discussion, irradiation of **1a** with $\lambda > 380$ nm gave extremely high selectivity with only small amounts of byproducts (Figure 6, bottom frame). As in the previous experiment, red solids slowly turned white while microscopic analysis revealed no apparent intervention of fluid phases. The importance of the crystalline environment on the selectivity of the reaction was also shown by comparison of the results obtained in crystals with $\lambda > 380$ nm with those from experiments carried out with amorphous solid samples. The latter samples were prepared by melting crystals of **1a** and rapidly quenching the melt in a liquid N_2 bath. The vitreous samples were treated in an identical manner as polycrystalline

(31) For examples of cis−trans isomerization in solids see: (a) Bregman, J.; Osaki, K.; Schmidt, G. M. J.; Sonntag, F. I. *J. Chem. Soc.* **1964**, 2021−2030. (b) Griffin, G. W.; O'Connel, E. J.; Kelliher, J. M. *Proc. Chem. Soc.* **1964**, 337. (c) Saigo, K. *Bull. Chem. Soc. Jpn.* **1996**, *69*, 779−784. (d) Kinbara, K.; Kai, A.; Maekawa, Y.; Hashimoto, Y.; Naruse, S.; Hasegawa, M.; Saigo, K. *Mol. Cryst. Liq. Cryst.* **1996**, *276*, 141−151.

Scheme 7

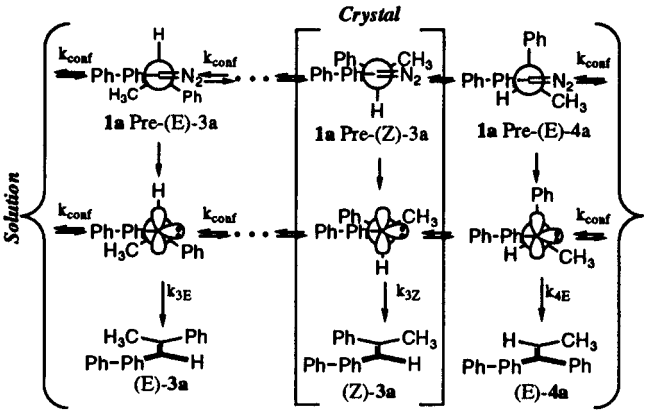

samples irradiated with the 380 nm cutoff filter. After 3 h of photolysis, 72% of the diazo was converted, and the samples were analyzed. The relative yields of (*E*)-**3a**, (*Z*)-**3a**, and (*E* + *Z*)-**4a** were 29%, 51%, and 20% (3% + 16%), respectively.

Irradiation and microscopic examination of single crystal specimens was carried out with $\lambda > 380$ nm. Single crystalline plates of *ca*. 0.5 × 2 × 3 mm were fixed onto a thin film of apiezon grease on a glass surface with care that no other crystal faces were contaminated. After only 15 min of irradiation, the crystals developed superficial fractures along the long crystal axis. After 0.5 h of irradiation, the ruby-red plates started to display a white coating inhomogeneously distributed over the crystal surface. Continued irradiation led to cloudy white crystals with some longitudinal fractures. While a small amount of a fine white powder observed along the periphery of irradiated crystals suggests the possibility of micro explosions to release trapped nitrogen, dissolution of crystals at the end of the experiments displayed a vigorous evolution of nitrogen gas.

(5) Solid-State Reaction Mechanism. EPR detection of carbene **2a** was accomplished with several single-crystal specimens that had their long axis aligned perpendicular to the magnetic field. Very long-lived signals (hours) covering a field width of *ca*. 4000 G were observed after the sample was exposed for 30 s to the output of a filtered 1 kW Oriel lamp at 77 K. Signals disappeared upon warming to ambient temperatures but could be obtained upon further exposure, and the cycle could be repeated. Analysis of the solid-state reaction by fluorescence detection showed that the carbene is stable for hours at 77 K but the fluorescence of stilbenes **3a** grows in rapidly at ambient temperatures. A detailed kinetic analysis as a function of temperature is currently in progress.

These results confirm that formation of (*Z*)-**3a** in the solid state occurs via the intermediacy of a carbene, **2a**, which undergoes a stereoselective 1,2-H shift. It is consistently agreed that carbene 1,2-H shifts have highly demanding transition states where the migrating hydrogen must overlap with the empty p-orbital of the sp^2-hybridized carbene carbon (Scheme 7).[32]

We propose that reaction control originates from the conformation of the reactant as determined by crystallization and from the structural barriers imposed by the crystal lattice that prevent conformational equilibrium and ensure a very high similarity between the diazo, the carbene, the transition state, and the final product. A Newman representation of several conformers of **1a** and **2a** along with a projection of their corresponding products in Scheme 7 makes a good graphical representation of this proposal. While all conformers may be available in solution media, only one is relevant in the solid state. In addition to individual activation energies, which are expected to be low,[33] product ratios in solution are determined by a subtle balance of conformational populations and isomerization rates, as well as singlet−triplet populations and intersystem crossing rates. Further complications occur in solution due to contributions from excited-state reactivity.[7] In contrast, in the solid-state reaction, the structure of the reactant and the rigidity of the crystal lattice make many of these arguments less important by restricting the structural possibilities of the reaction.

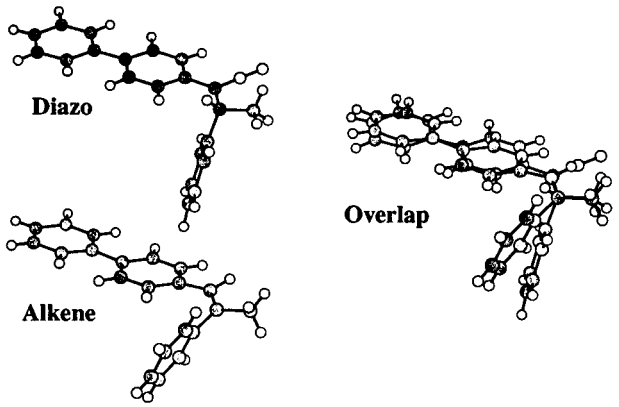

Figure 7. X-ray structures of compound **1a**, its major solid-state photoproduct (*Z*)-**3a**, and their overlap.

In spite of a high concentration of diazo compound, crystals of **1a** prevent intermolecular processes that are common in concentrated solutions. The packing diagram of **1a** (Figure 1) explains the absence of intermolecular reactions that would give rise to azines or alkenes by reaction of carbenes with diazo compounds[34] or with themselves,[35] respectively. The distance between prospective carbene carbons and the terminal diazo nitrogen of the closest neighboring molecules (required for azine formation) is 6.35 Å. The closest distance between prospective carbene carbons (required for alkene formation) is 7.38 Å. Not only are these distances too long but the diazo groups of adjacent molecules do not have the required alignment for bimolecular reactions to occur. A close packing structure prevents molecular diffusion and rotation, which could lead to these products.

After obtaining the X-ray structure of photoproduct (*Z*)-**3a** and comparing it with that of diazo **1a**, we confirmed that the pictorial representation of the solid state reaction in Scheme 7 is supported beyond our most optimistic expectations. For our analysis we have assumed that carbene **2a** can only experience relatively minor relaxation so that in the crystal it retains the overall shape of the precursor. Thus, the X-ray molecular structure of diazo compound **1a** corresponds closely to that of conformer **1a** Pre-(*Z*)-**3a** in Scheme 7. This structure possesses the biphenyl and phenyl groups gauche to each other with the α-hydrogen deviating from the expected orientation by *ca*. 37°. Side-by-side comparison and overlap of the X-ray structures of the reactant and the product also shows outstanding similarities (Figure 7). With the exception of the migrating hydrogen, in going from the reactant to the product, there are only small atomic displacements and the solid state reaction effectively constitutes a least motion process. A recent computational

(32) (a) Evanseck, J. D.; Houk, K. N. *J. Phys. Chem.* **1990**, *94*, 5518−5523. (b) Schaefer, H. F., III. *Acc. Chem. Res.* **1979**, *12*, 288−296. (c) Kyba, E. P.; John, A. M. *J. Am. Chem. Soc.* **1977**, *99*, 8330−8332.

(33) Sugiyama, M. H.; Celebi, S.; Platz, M. S. *J. Am. Chem. Soc.* **1992**, *114*, 966−973.

(34) Example of carbenes reacting with diazo compounds: Griller, D.; Majewski, M.; McGimpsey, W. G.; Nazran, A. S.; Scaiano, J. C. *J. Org. Chem.* **1988**, *53*, 1550−1553.

(35) Example of carbenes reacting with themselves: (A) Zimmerman, H. E.; Paskovich, D. H. *J. Am. Chem. Soc.* **1964**, *86*, 2149−2160. (b)-Nazran, A. S.; Lee, F. L.; Gabe, E. J.; Lepage, Y.; Northcote, D., J.; Park, J. M.; Griler, D. *J. Phys. Chem.* **1984**, *88*, 5251−5254.

Scheme 8

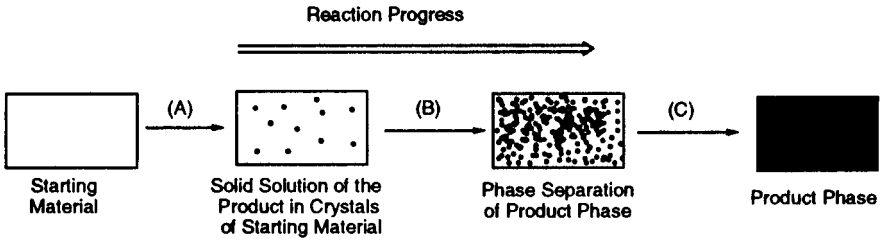

analysis based on the calculation of steric energies along the *ab initio* gas-phase reaction coordinate suggests that planarization during rehybridization of the α-carbon and a small displacement of the phenyl group do not cause strongly adverse nonbonding interactions between the reactant and the crystal lattice.[36]

(6) Study of Crystal Changes as a Function of Reaction Progress. Organic reactions in crystals may be extremely complex non-linear processes.[37] While crystal packing and molecular structure control the reactivity and the selectivity of reaction, changes in composition due to reaction may affect the structure of the crystal. It is not uncommon that high selectivities and specificities may only be observed at low conversion values because of destruction of the crystal lattice. In this context, the solid-state transformation of **1a** into (*Z*)-**3a** is remarkable because the selectivity of the reaction is maintained to nearly quantitative conversion values (see Figure 6). We have carried out a thorough spectroscopic and thermal analysis to elucidate the nature of the phase changes occurring in this reaction.

The foundation for understanding the consequences of product accumulation in solid-state reactions was briefly laid down by Schmidt in reference to numerous examples of cinnamic acid derivatives.[38] Schmidt proposed that product molecules go into solid solution in the lattice of the reactant until they reach their solubility limit, when they separate into their own phase (Scheme 8). It should be pointed out that separation of a liquid phase (melting) is expected to occur if the temperature of the reaction is above the eutectic temperature of the reactants and the products. By careful spectroscopic and thermal analysis we have recently observed that efficient solid-state photochemical reactions may involve a solid solution present only in a steady state.[30,38] An alternative, but infrequent, situation involves the so-called single crystal-to-single crystal, or topotactic transformations.[39] These are ideal situations where crystals of the reactant smoothly transform into crystals of the product by means of a solid solution that covers their entire composition diagram. The crystal structure of the reactant and the crystal structure of the product in this case are isomorphic, and they constitute a single phase with the greatest potential for reaction control.

The X-ray structures of **1a** and (*Z*)-**3a** cannot be the end points of a continuous phase involving a solid solution,[40] and the solid state reaction of **1a** cannot be topotactic. Although both compounds crystallize in space group $P2_1/c$ their packing arrangements are different (see Figures 1 and 2). Compound

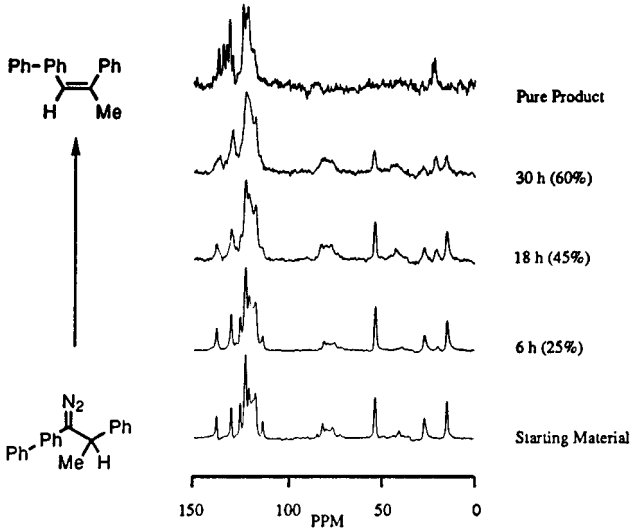

Figure 8. ^{13}C CPMAS spectra of crystalline samples of **1a** (bottom) and (*Z*)-**3a** (top) along with partially reacted samples to 25, 45, and 60% conversion (as labeled).

1a crystallizes with only one molecule per asymmetric unit while (*Z*)-**3a** crystallizes in two different conformers that differ in the torsion angle of their biphenyl substituents, which are 1.6° and −33.6°, respectively. The high molecular similarity between **1a** and one conformer of (*Z*)-**3a** is shown in Figure 7. A similar structural match may be obtained in all respects, except for the relatively soft biphenyl torsion, between **1a** and the other conformer of (*Z*)-**3a**.[41] We propose that the excellent structural overlap of molecules of **1a** and (*Z*)-**3a** allows for a high solid-state solubility of the product in crystals of the reactant, but the poor structural overlap of their packing arrangements prevents them from being part of a continuous solid phase. It was our goal to determine whether the solid phase of "as formed" (*Z*)-**3a** is the same as or different from that obtained after recrystallization.

Spectral analysis of the solid-state reaction was carried out as a function of conversion by ^{13}C CPMAS NMR.[42] Spectra were collected with the TOSS sequence for spinning sideband suppression. A stack plot with spectra of the starting material (bottom), the recrystallized product (top), and three intermediate values (25, 45, and 60% conversion) is shown in Figure 8. The solid-state spectrum of **1a** qualitatively matches the spectrum obtained in solution. Seven out of 18 nonequivalent aromatic signals are resolved in the range between 120 and 145 ppm, while the diazo, methine, and methyl carbons resonate at *ca.* 60.1, 33.6, and 21.6 ppm, respectively. The spectrum of the product [(*Z*)-**3a**] on the top of Figure 8 displays eight aromatic signals corresponding to 28 aromatic and vinylic carbons of

(36) Keating, A. E.; Shin, S. H.; Houk, K. N.; Garcia-Garibay, M. A. *J. Am. Chem. Soc.*, in press.

(37) Garcia-Garibay, M. A.; Constable, A. E.; Jernelius, J.; Choi, T.; Cizmeciyan, D.; Shin, S. H. In *Physical Supramolecular Chemistry*; Echegoyen, L., Kaifer, A., Eds.; Kluwer Academic Publishers: Dordrecht, 1996; pp 289−312.

(38) Schmidt, G. M. J. *J. Chem. Soc.* **1964**, 2014−2021.

(39) (a) Wegner, G. *Pure Appl. Chem.* **1977**, *49*, 443−454. (b) Thomas, J. M. *Nature* **1981**, *289*, 633. (c) Theocharis, C. R.; Jones, W. In *Organic Solid State Chemistry*; Desiraju, G., Ed.; Elsevier: Amsterdam, 1987; pp 47−67.

(40) Kitaigorodski, A. I. *Mixed Crystals*; Springer Verlag: Berlin, 1984.

(41) It has been proposed that planar biphenyl is a time-average structure: Baudour, J. L. *Acta Crystallogr. B* **1991**, *47*, 935−949.

(42) (a) Fyfe, C. A. *Solid State NMR for Chemists*; CFC Press: Guelph, Ontario, 1983. (b) Yannoni, C. S. *Acc. Chem. Res.* **1982**, *15*, 201−208. (c) Schaefer, J.; Stejskal, E. O. *Top. Carbon-13 NMR Spectrosc.* **1979**, *3*, 283−324.

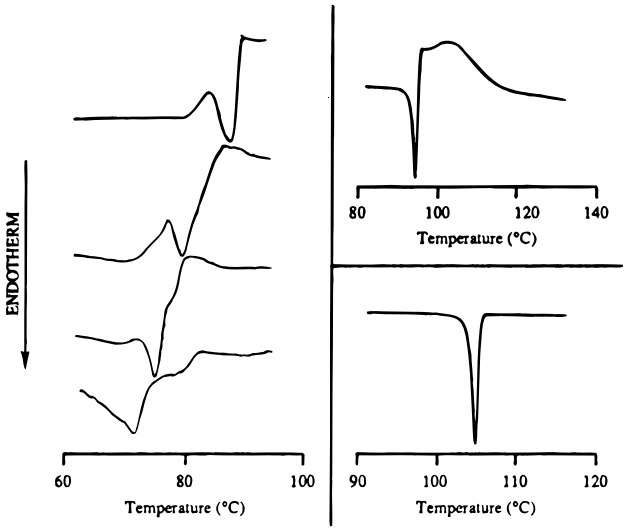

Figure 9. DSC traces of crystalline samples of **1a** (upper right), (*Z*)-**3a** (lower right), and partially reacted samples to 25, 45, and 60% conversion (left).

the two distinct molecules in the crystal of (*Z*)-**3a**. Signals corresponding to the methyl groups (one per conformer) appear resolved at 29.0 and 27.8 ppm, respectively.

The progress of the reaction is clearly visible in spectra obtained at intermediate stages. As the reaction proceeds, signals of the reactant show increasing broadening while signals corresponding to the product start to grow in. Interestingly, product signals are also quite broad and not at all recognizable as those of recrystallized (*Z*)-**3a** at the top of the figure. The spectra of partially converted **1a** cannot be reproduced by linear additions of spectra corresponding to the reactant and the products. These results contrast very sharply with previous observations in our group where a solid-state reaction forms a separate solid phase of the product with clear ^{13}C NMR signals that grow sharp from the beginning.[30,38] We also noticed that the spectra continue evolving as a function of conversion, suggesting that solid-state reaction of **1a** proceeds by a continuous-phase mechanism rather than by a phase-separation mechanism. While similar qualitative observations were made by solid-state FT-IR (not shown), confirmation of this may be obtained by differential scanning calorimetry (DSC).

DSC measurements that paralleled the ^{13}C CPMAS NMR spectra were carried out with pure and partially reacted samples (Figure 9). The thermogram of the reactant is characterized by a sharp melting endotherm at 94 °C followed by a strong exotherm assigned to the thermal denitrogenation of the diazo compound. It is interesting that no thermal decomposition occurs below the melting point with heating rates between 2 and 10°/min. Constant temperature runs with samples maintained at 90 °C (which is only 4 °C below their melting point) decomposed after 12 min, suggesting a high thermal stability for compound **1a** when in the crystalline state. Crystals of product (*Z*)-**3a** display a sharp melting endotherm at 103 °C with no other transitions that may be assigned to liquid crystalline phases, which are relatively common for biphenylyl-substituted compounds.

The thermal behavior of partially reacted samples of **1a** is extremely complex but quite illustrative and interesting. First of all, the lack of a eutectic transition clearly implies that reaction occurs through a continuous solid phase. Secondly, the absence of melting transitions below *ca*. 60 °C indicates that the reaction proceeds entirely in the solid state. Thirdly, even at a point where only small quantities of (*Z*)-**3a** may be present, it is noticed that the exothermic transition comes to

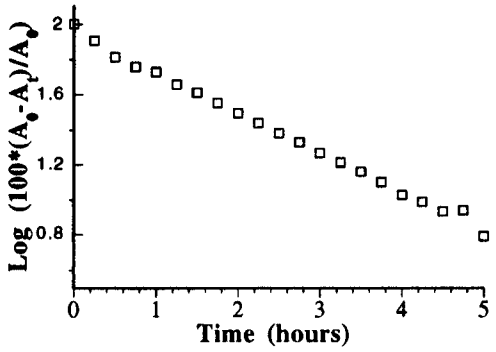

Figure 10. First-order plot for irradiation of microcrystalline samples of **1a** as a function of time at 25 °C with $\lambda > 380$ nm. A_0 and A_t refer to the IR absorbance values at the diazo stretch at time = 0 and time = *t*.

precede the melting endotherm. The latter observation suggests that small quantities of product disturb the crystal lattice of **1a** to the extent that it no longer stabilizes the diazo compound. It also seems from these results that a thermal reaction in the solid state may be possible if carried out with care (to prevent melting), and work is currently in progress to determine the selectivity of the thermal reaction.

From the above results one may conclude that the solid-state reaction of **1a** proceeds in a single phase and that the solid phase of "as formed" (*Z*)-**3a** is not related to that obtained after recrystallization. Since the selectivity of the solid state reaction for (*Z*)-**3a** remains unaltered, regardless of the composition of the solid, we propose that the "as formed" product phase retains most of the structural properties of the initial phase of the reactant. Although some order may be lost as the reaction proceeds, we conclude that the conformation of the diazo compound and its environment retain the influences that dictate the course of the solid-state reaction.

Experiments with microcrystalline samples in optically clear KBr matrices with constant illumination at $\lambda > 380$ nm also give evidence of a relatively homogeneous process with excellent apparent first-order plots. Figure 10 was obtained with conversion values calculated from FT-IR absorbance of the diazo signal. It is expected that the slope of the plot should depend on the number of quanta absorbed, given by the intensity of the irradiating beam, and on the quantum yield of the reaction. The data show that the apparent rate of disappearance of **1a** is the same at the early stages of the reaction and at the end. This is not always the case with solid-state reactions. Some become less efficient as the product accumulates, and similar plots bend upward.[43] Other reactions appear to become more efficient, as their first-order plots bend downward, suggesting that melting may occur as the reaction goes on.

III. Conclusions

We have shown that the crystalline solid state may control the reactivity of aryldiazoalkanes to levels that have not been accomplished with any other media. Although we have also shown strong evidence for a carbene intermediate, we may not discount the partial contribution to product formation of an excited-state reaction of the diazo compound. We have suggested that reaction control in the crystal derives from conformational factors that determine orbital alignment and from environmental factors that maintain a strong structural similarity between the reactant, the intermediate, the transition state and the final product. Spectroscopic and thermal analysis of changes

(43) Garcia-Garibay, M. A. PhD Thesis, University of British Columbia, 1988.

in the crystalline solid as a function of reaction progress suggest a continuous phase. With spectroscopic, thermal, and chemical (cis−trans isomerization) measurements it was shown that the solid accumulated at the end of the reaction is different from that obtained after recrystallization. Finally, it was clearly demonstrated that the importance of experimental conditions (temperature, wavelength) on the selectivity of solid-state reactions should not be underestimated.

IV. Experimental Section

We describe here the procedures for solution- and solid-state experiments. Instrumentation details, the preparation and characterization of compounds shown in Schemes 3 and 4, and photoisomerization experiments are described in detail in the Supporting Information.

Solution Photolysis. Approximately 1 mg of **1a** was dissolved in 1 mL of solvent. The solution was placed in an NMR tube, and N_2 gas was bubbled through the solution for 20 min to deoxygenate the sample. Photolysis was carried out in an ice bath (0 °C) with a 380 nm cutoff filter. Samples were irradiated for 30 min after which time the characteristic red color of **1a** had disappeared. Upon completion of photolysis, dimethyl acetylenedicarboxylate (DMAD) was added to react with any remaining **1a**. GC analysis revealed the composition of the product mixture, and the results are shown in Table 2.

Microscale Solid-State Photolysis. A sample of 20 mg of **1a** was ground into a fine powder and mixed with 5 mg of ground crystals of triphenylmethanol, which served as a standard to determine extent of conversion of **1a**. Powdered samples were placed between two microscope slides in a polyethylene bag immersed in an ice bath (0 °C). Photolyses were performed with 350 and 380 nm cutoff filters. Approximately 1 mg of the irradiated sample was removed for analysis every 15−60 min. The removed portion was dissolved in diethyl ether, and DMAD was added to react with unreacted **1a**. The resulting solution was analyzed by GC. The results of these experiments are shown in Figure 6. Microscale photolysis was also carried out with an amorphous solid sample of **1a**. The sample was obtained by grinding, fast melting, and liquid N_2 quenching of 5 mg of **1a**. The glassy material thus obtained was sandwiched between two microscope slides. The slides were clamped together and irradiated for about 3 h in an ice bath (0 °C) with the 380 nm filter. The sample was removed, dissolved in ether, and analyzed by GC. The yields of (*Z*)-**3a**, (*E*)-**3a**, and **4a** (*E* and *Z* isomers) were 51%, 29%, and 20% (3% + 16%), respectively.

Medium-Scale Solid-State Photolysis. A sample of 400 mg of **1a** was ground into a fine powder. This powder was placed on a watch glass, covered with a 380 nm filter, and photolyzed. At varying time intervals (15−60 min) irradiation was stopped and the sample removed for analysis. A ^{13}C CPMAS solid state NMR was obtained after each photolysis period. The sample was returned to the photolysis setup for further irradiation after 7 mg of the sample was removed. About 5 mg of those were used for DSC (differential scanning calorimetry) and 1 mg for solid-state FT-IR in a KBr matrix. The final 1 mg of sample was dissolved in diethyl ether and treated with DMAD to react with any remaining **1a**. The resulting solution was analyzed by GC to determine the products of photolysis. At the end of the experiment, the remaining sample was recrystallized from hexanes to give crystals of pure (*Z*)-**3a**. The results form this experiments are shown in Figures 8 (CPMAS ^{13}C NMR) and 9 (DSC). Yields determined by FT-IR were consistent with yields obtained by GC.

Acknowledgment. Support by the National Science Foundation and the Petroleum Research Fund, administered by the American Chemical Society, is gratefully acknowledged. The National Science Foundation is also acknowledged for a graduate research fellowship to A.E.K.

Supporting Information Available: Experimental description of the preparation and characterization of compounds in Schemes 3 and 4. Description of photoisomerization experiments in solution and in the solid state. Details of X-ray data collection and structure refinements of compounds **1a** and **3a**, solution, and CPMAS solid-state ^{13}C NMR data of compounds **1a** and **3a** (11 pages). See any current masthead page for ordering and Internet access instructions.

JA9633225